2024 IEEE 63rd Conference on Decision and Control (CDC)
December 16-19, 2024. MiCo, Milan, Italy

Enhanced Battery State Estimation: Part 2 – Reverse Sensitivity Analysis and Electrode Lithium-ion Observer

Sara Sepasiahooyi and Shu-Xia Tang

2024 IEEE 63rd Conference on Decision and Control (CDC) | 979-8-3503-1633-9/24/$31.00 ©2024 IEEE | DOI: 10.1109/CDC56724.2024.10885930

***Abstract*— In lithium-ion batteries, the lithium concentration within the electrolyte is one of the key variables. This paper explores how variations in electrolyte concentration at the terminal boundaries affect different battery parameters through a reverse sensitivity analysis. Analytical derivation is employed as the method, which is universally applicable to various battery types with different parameters. By performing a reverse sensitivity analysis on a $LiFePO_4$ battery cell under an Urban Dynamometer Driving Schedule (UDDS) current profile, the most and least sensitive parameters are identified. These findings are valuable for Part 1 of this study, where observers are introduced to estimate the electrolyte lithium concentration. The designed observers require the lithium-ion concentration at the terminal boundaries, which is difficult to measure directly. Thus, based on the results of this reverse sensitivity analysis, the most suitable measurable parameter can be identified to infer the electrolyte lithium concentration at the boundaries for application in Part 1.**

***Index Terms*— Li-ion battery; Reverse sensitivity analysis; Electrode concentration; Electrolyte resistance.**

I. Introduction

Lithium-ion batteries have become ubiquitous due to their extensive applications. Investigations into battery parameters and their impact on battery aging could significantly contribute to advancements in the battery industry [1]. The battery electrochemical model includes many parameters, each with varying degrees of sensitivity to the primary variables. This variability introduces uncertainties in overall predictions [2]. These uncertainties can be reduced by conducting sensitivity analyses to identify relevant target variables and the main sources of uncertainty [3].

In recent years, several sensitivity analysis studies on lithium-ion batteries have been conducted. In [4], the Fisher Information Matrix was utilized to find the sensitivity of terminal voltage, as the model output, to different electrochemical model parameters. Zhang et al. In [5], Monte Carlo simulations were used to conduct sensitivity analysis on 14 factors related to the safety of a battery cell under stressed conditions. In [6] and [7], an analytical derivation approach was employed to explore terminal voltage sensitivity to various battery parameters and state-of-health indicators, respectively. In this study, an analytical derivation approach is employed, which provides precise results by directly utilizing mathematical equations, making it more time-efficient and less computationally intensive than the Monte Carlo method, which relies on extensive random sampling and simulations. In most studies, the sensitivity of terminal voltage to battery parameters is commonly explored, while other parameters, such as lithium concentration, can also serve as target variables, offering valuable insights. The concentration of lithium ions in the electrolyte phase stands out as a key element, as it facilitates ion conduction and significantly affects battery capacity and cycle aging [8]. In this paper, reverse sensitivity analysis is performed on electrolyte conductivity, diffusion coefficient, and resistance to lithium concentration to quantify how variations in electrolyte lithium concentration influence these parameters. Even though this study stands alone, its findings can significantly benefit Part 1 of this study [9] by determining the most appropriate measurable parameter for obtaining electrolyte lithium concentration at the boundaries for designing the electrolyte observer. The primary contributions of this research include:

- Unlike the vast majority of sensitivity analysis studies, which use numerical approaches [3], [10], this study employs an analytical derivation method for sensitivity analysis. To the best of our knowledge, analytical derivation for sensitivity analysis has only been utilized in [6] and [7]. The analytical method is a precise and generic approach applicable to all types of batteries under various current profiles.
- The Single Particle Model with electrolyte (SPMe) dynamics is utilized as the battery model, known for its superior accuracy at high C-rates compared to the SPM.
- Global sensitivity analysis is conducted to assess the overall reverse sensitivity of electrolyte concentration to electrolyte conductivity, the electrolyte diffusion coefficient, and electrolyte resistance across the entire parameter space. This analysis helps identify which parameters have the most significant impact on the overall model behavior.

The remainder of this paper is organized as follows: Section II conducts a reverse sensitivity analysis of electrolyte lithium-ion concentration at the boundary to various parameters. Section III demonstrates simulation results on a $LiFePO_4$ battery cell. In Section IV, electrolyte lithium-ion concentration observers are proposed, employing the results of the reverse sensitivity analysis. Section V-A explains the electrode estimator and demonstrates how this study contributes to achieving greater accuracy and enhancing the electrode lithium-ion observer, followed by the conclusion and a discussion of future work in Section VI.

S. Sepasiahooyi and S.-X. Tang (correspondening author) are with the Department of Mechanical Engineering, Texas Tech University, Lubbock, USA. ssepasia@ttu.edu, shuxia.tang@ttu.edu.

Authorized licensed use limited to: Texas Tech University. Downloaded on March 19,2025 at 15:03:30 UTC from IEEE Xplore. Restrictions apply.

II. Reverse sensitivity analysis of electrolyte lithium concentration at the boundaries

In this section, reverse sensitivity analysis is conducted to identify the least effective parameter influencing the electrolyte lithium concentration at the terminal boundaries $c_e^{\pm}(t,0^{\pm})$, which will then be employed in the design of subsequent observers. Among the various parameters in the electrochemical battery model, electrolyte conductivity $\kappa_e^{\pm}$, diffusion coefficient in the electrolyte $D_e^{\pm}$, and electrolyte resistance $R_e^{\pm}$ are measurable quantities that correlate with the electrolyte lithium concentration.

A. Reverse sensitivity analysis of electrolyte lithium concentration at the terminal boundaries $c_e^{\pm}(t,0^{\pm})$ electrolyte diffusion coefficient to $D_e^{\pm}(t,0^{\pm})$

The electrolyte diffusion coefficient $D_e^{\pm}$ determines the rate at which lithium ions migrate between the electrodes [11]. The Einstein relation [12] reveals the correlation between the diffusion coefficient in the electrolyte $D_e^{\pm}(t,0^{\pm})$ and the concentration of lithium ions in the electrolyte $c_e^{\pm}(t,0^{\pm})$ at the terminal boundaries:

$$D_e^{\pm}(t,0^{\pm}) = \frac{k_B T \kappa_e^{\pm}(c_e^{\pm}(t,0^{\pm}))}{e^2 N_A c_e^{\pm}(t,0^{\pm})}, \tag{II.1}$$

where k_B is the Boltzmann constant. T and $\kappa_e^{\pm}(c_e^{\pm}(t,0^{\pm}))$ are temperature and electrolyte conductivity at the terminal boundaries, respectively. e is the elementary charge and N_A is the Avogadro constant. The reverse sensitivity of lithium-ion concentration $c_e^{\pm}(t,0^{\pm})$ to the diffusion coefficient in the electrolyte at the boundaries $D_e^{\pm}(t,0^{\pm})$ is derived as follows:

$$\frac{\partial D_e^{\pm}(t,0^{\pm})}{\partial c_e^{\pm}(t,0^{\pm})} = \frac{-k_B T \kappa_e^{\pm}(c_e^{\pm}(t,0^{\pm}))}{e^2 N_A (c_e^{\pm}(t,0^{\pm}))^2}.$$

B. Reverse sensitivity analysis of electrolyte lithium concentration at the terminal boundaries $c_e^{\pm}(t,0^{\pm})$ to electrolyte conductivity $\kappa_e^{\pm}(t,0^{\pm})$

The electrolyte conductivity in lithium-ion batteries determines the ability of lithium ions to move freely within the electrolyte solution. The Einstein relation (II.1) expresses the link between the electrolyte concentration $c_e^{\pm}(t,0^{\pm})$ and the electrolyte conductivity $\kappa_e^{\pm}(t,0^{\pm})$ at the boundaries. The analytical derivation from $c_e^{\pm}(t,0^{\pm})$ to $\kappa_e^{\pm}(t,0^{\pm})$ is as follows:

$$\frac{\partial \kappa_e^{\pm}(t,0^{\pm})}{\partial c_e^{\pm}(t,0^{\pm})} = \frac{e^2 N_A D_e^{\pm}(t,0^{\pm})}{T k_B}. \tag{II.2}$$

C. Reverse sensitivity analysis of electrolyte lithium concentration at the terminal boundaries $c_e^{\pm}(t,0^{\pm})$ to electrolyte resistance $R_e^{\pm}(t)$

Electrolyte resistance is a critical parameter in lithium-ion batteries, as higher resistance hinders lithium-ion movement, reducing conductivity and slowing charge-discharge rates. The electrolyte resistance in the negative and positive electrodes is described as follows [7]:

$$R_e^{\pm}(t) = \frac{L^{\pm}}{2A\kappa_e^{\pm,\text{eff}}(c_e^{\pm}(t,0^{\pm}),\varepsilon_e^{\pm}(t))}, \tag{II.3}$$

where $L^{\pm}$ denotes the thickness of the negative and positive electrodes. A is the electrode area, and $\kappa_e^{\pm,\text{eff}}(c_e^{\pm}(t,0^{\pm}),\varepsilon_e^{\pm}(t)) = \kappa_e^{\pm}(c_e^{\pm}(t,0^{\pm}))(\varepsilon_e^{\pm}(t))^{1.5}$ represents the effective conductivity of the electrolyte. $\varepsilon_e^{\pm}(t)$ is the volume fraction of electrolyte phase. By combining (II.3) and (II.1), the reverse sensitivity of electrolyte lithium concentration $c_e^{\pm}(t,0^{\pm})$ to the electrolyte resistance at the boundaries $R_e^{\pm}(t)$ is derived as:

$$\frac{\partial R_e^{\pm}(t)}{\partial c_e^{\pm}(t,0^{\pm})} = \frac{L^{\pm} k_B T}{2Ae^2 D_e^{\pm} N_A (c_e^{\pm}(t,0^{\pm}))^2}.$$

Remark: Reverse sensitivity analysis is typically performed on the boundaries between the electrode and the current collector $c_e^{\pm}(t,0^{\pm})$. It can also be extended to the boundaries between the separator and the electrodes $c_e^{\pm}(t,L^{\pm})$.

III. Reverse Sensitivity Analysis on a $LiFePO_4$ Battery Cell

In this section, an example of reverse sensitivity analysis is performed on a $LiFePO_4$ battery cell with a rated capacity of 2.3 Ah under a UDDS current profile, as shown in Fig. 1 [13]. The simulation was conducted using MATLAB on a MacBook Pro equipped with an Apple M2 CPU and 8 GB of RAM, taking approximately 3 minutes to complete. The electrochemical parameters used in the simulation, detailed in Table I, are taken from [14]. Relation of electrolyte lithium

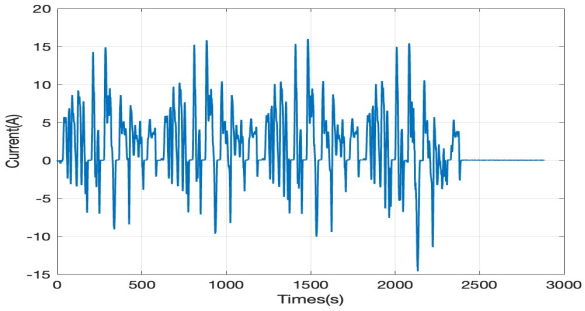

Fig. 1: UDDS current profile

concentration with electrolyte conductivity is determined as follows [15]:

$$\kappa_e^{\pm}(c_e^{\pm},T) = 1.12\times10^{-4}(-8.2488 + 0.053248T - 2.9871 \times 10^{-5}T^2 + 0.26235(c_e^{\pm}) - 9.3063\times10^{-3}T + 8.069 \times 10^{-6}c_e^{\pm}T^2 + 0.220022(c_e^{\pm})^2 - 1.765\times10^{-4}(c_e^{\pm})^2T).$$

The relation between electrolyte lithium concentration and electrolyte diffusion coefficient is formulated as follows [15]:

$$D_e^{\pm}\left(c_e^{\pm},T\right) = 10^{\left(-4.43-\left(\frac{54}{T-229-0.005c_e^{\pm}}\right)-0.0022c_e^{\pm}\right)-4}.$$

The temperature is kept constant at $T = 298$ K. Fig. 2 and Fig. 3 demonstrate the reverse sensitivity of the electrolyte concentration $c_e^{\pm}(t,0^{\pm})$ to the electrolyte conductivity at the boundaries $\kappa_e^{\pm}(t,0^{\pm})$ in the negative and positive electrodes, respectively. Figs. 4 and 5 illustrate the reverse sensitivity of electrolyte lithium concentration $c_e^{\pm}(t,0^{\pm})$ to the electrolyte diffusion coefficient $D_e^{\pm}(t,0^{\pm})$ at the boundaries within the

Authorized licensed use limited to: Texas Tech University. Downloaded on March 19,2025 at 15:03:30 UTC from IEEE Xplore. Restrictions apply.

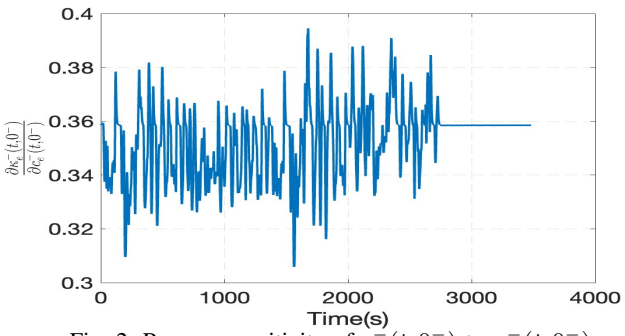

Fig. 2: Reverse sensitivity of $c_e^-(t,0^-)$ to $\kappa_e^-(t,0^-)$

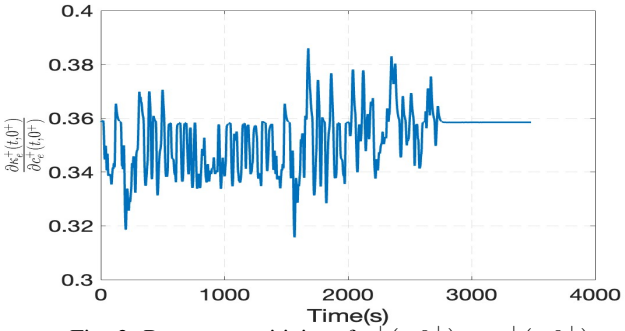

Fig. 3: Reverse sensitivity of $c_e^+(t,0^+)$ to $\kappa_e^+(t,0^+)$

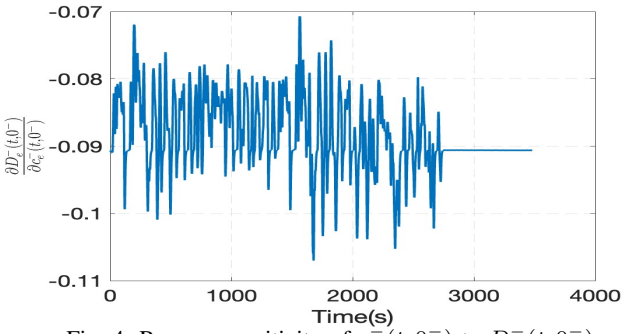

Fig. 4: Reverse sensitivity of $c_e^-(t,0^-)$ to $D_e^-(t,0^-)$

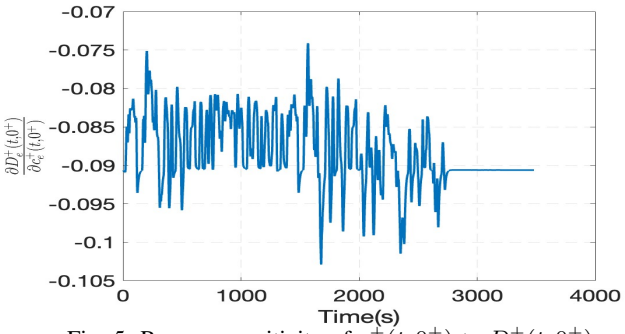

Fig. 5: Reverse sensitivity of $c_e^+(t,0^+)$ to $D_e^+(t,0^+)$

negative and positive electrodes, respectively. The reverse sensitivity of the electrolyte concentration $c_e^{\pm}(t,0^{\pm})$ to the electrolyte resistance at the boundaries $R_e^{\pm}(t,0^{\pm})$ in negative and positive electrodes are plotted in Fig. 6 and Fig. 7, respectively. It can be observed that the electrolyte concentration at the boundaries $c_e^{\pm}(t,0^{\pm})$, is more sensitive to the electrolyte conductivity $\kappa_e^{\pm}(t,0^{\pm})$ and less sensitive to the electrolyte resistance $R_e^{\pm}(t)$.

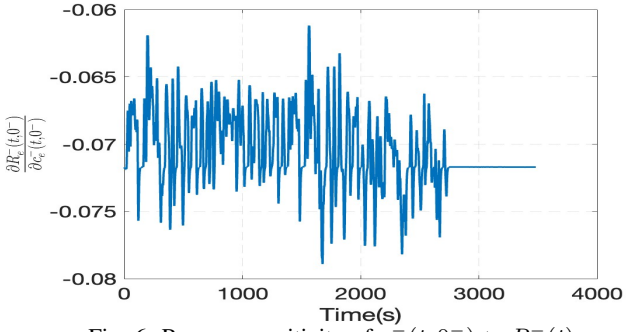

Fig. 6: Reverse sensitivity of $c_e^-(t,0^-)$ to $R_e^-(t)$

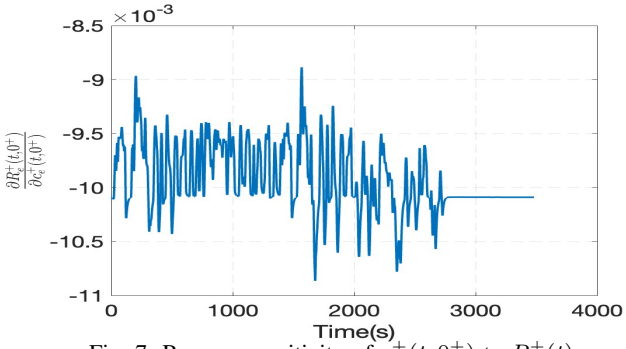

Fig. 7: Reverse sensitivity of $c_e^+(t,0^+)$ to $R_e^+(t)$

IV. Electrolyte Observer

The results of the reverse sensitivity analysis are utilized in the proposed closed-loop electrolyte lithium concentration observers in Part 1 [9]. In these observers, the electrolyte lithium concentration at the terminal boundaries $c_e^{\pm}(t,0^{\pm})$, is required for injecting the state estimation error at the boundaries. However, measuring $c_e^{\pm}(t,0^{\pm})$ is challenging. Therefore, a measurable parameter correlated with $c_e^{\pm}(t,0^{\pm})$ is needed to determine $c_e^{\pm}(t,0^{\pm})$. Through reverse sensitivity analysis, measurable parameter that is less sensitive and more robust to variations in $c_e^{\pm}(t,0^{\pm})$ is identified. For a $LiFePO_4$ battery cell, the electrolyte resistance $R_e^{\pm}(t)$ stands out as the most suitable measurement for finding the electrolyte lithium concentration at the boundaries due to its minimal variations. Through the measurement of bulk resistance, Electrochemical Impedance Spectroscopy (EIS) effectively quantifies electrolyte resistance within the system [16]. While simulation results may vary for different types of batteries, and other measurable parameters may be selected to obtain electrolyte lithium concentration at the boundaries, the proposed observer design remains consistent.

Authorized licensed use limited to: Texas Tech University. Downloaded on March 19,2025 at 15:03:30 UTC from IEEE Xplore. Restrictions apply.

TABLE I: Electrochemical parameters of a 2.3 Ah $LiFePO_4$ battery.

Symbol	Description	Value
D_s^+	Diffusion coefficient of positive electrode [m^2/s]	5.9×10^{-18}
D_s^-	Diffusion coefficient of negative electrode [m^2/s]	3×10^{-14}
$D_e^{\pm}$	Diffusion coefficient of positive and negative electrode [m^2/s]	1.2×10^{-10}
ε_s^+	Volume fraction of positive electrode	0.374
ε_s^-	Volume fraction of negative electrode	0.580
ε_e^+	Volume fraction of electrolyte in positive electrode	0.2
ε_e^-	Volume fraction of electrolyte in negative electrode	0.426
$\varepsilon_e^{\text{sep}}$	Volume fraction of electrolyte in separator	0.360
κ_e^+	Electrolyte conductivity in positive electrode	100
κ_e^-	Electrolyte conductivity in negative electrode	0.78
t_c^0	Transference number	0.36
$c_e(0,x)$	Initial condition of electrolyte lithium concentration [mol m^{-3}]	1200

Remark 1. Note that measuring electrolyte resistance at the boundaries requires EIS, which is is an offline technique. Generally, EIS spectrum measurements at 60 frequencies ranging from 100 kHz to 0.1 Hz typically take 2 to 3 minutes to complete [17]. Incorporating the event-triggered concept into the observer facilitates the realization of this scheme, which is a topic for future work [18].

A. Electrolyte lithium concentration observers

For designing electrolyte observers, the following assumption is considered.

Assumption 1. *To simplify the observer design, the diffusion coefficient in the electrolyte phase, $D_e^{\pm}(c_e^{\pm}(t,x))$, is assumed to be constant.*

Note that the complexity of $D_{\text{e}}^{\pm}(c_e^{\pm}(t,x))$ is retained in the main part of this study.

A.1 Normalization of system

The normalized electrolyte lithium concentration within the negative electrode and the boundary conditions are presented as follows [9]:

$$\frac{\partial c_{\text{e}}^-(t,x)}{\partial t} = \frac{\partial^2 c_{\text{e}}^-(t,x)}{\partial x^2} + \frac{L^-(1-t_c^0)}{D_{\text{e}}^{-,\text{eff}}F} I(t), \tag{IV.1}$$

$$\frac{\partial c_{\text{e}}^-}{\partial x}(t,0^-) = 0, \tag{IV.2}$$

$$\frac{\partial c_e^-}{\partial x}(t,1^-) = \frac{-L^- c_e^-(t,1^-)}{P^*}, \tag{IV.3}$$

where $t > 0$ and $x \in (0,1)$, and P^* is the equilibrium point explained in Part 1 [9]. The normalized electrolyte lithium concentration in the positive electrode and its boundary conditions are as follows:

$$\frac{\partial c_{\text{e}}^+(t,x)}{\partial t} = \frac{\partial^2 c_{\text{e}}^+(t,x)}{\partial x^2} - \frac{L^+(1-t_c^0)}{D_{\text{e}}^{+,\text{eff}}F} I(t), \tag{IV.4}$$

$$\frac{\partial c_{\text{e}}^+}{\partial x}(t,0^+) = 0, \tag{IV.5}$$

$$\frac{\partial c_e^+}{\partial x}(t,1^+) = \frac{L^+ c_e^+(t,1^+)}{L^{\text{sep}} - P^*}. \tag{IV.6}$$

B. Electrolyte observer for the negative electrode

The observer for the electrolyte lithium concentration in the negative electrode is proposed as follows:

$$\frac{\partial \hat{c}_{\text{e}}^-}{\partial t}(t,x) = \frac{\partial^2 \hat{c}_{\text{e}}^-}{\partial x^2}(t,x) + \frac{L^-(1-t_c^0)}{D_{\text{e}}^{-,\text{eff}}F} I(t) + p_1(x)(c_{\text{e}}^-(t,0^-) - \hat{c}_{\text{e}}^-(t,0^-)), \tag{IV.7}$$

$$\frac{\partial \hat{c}_{\text{e}}^-}{\partial x}(t,0^-) = p_{10}(c_{\text{e}}^-(t,0^-) - \hat{c}_{\text{e}}^-(t,0^-)), \tag{IV.8}$$

$$\frac{\partial \hat{c}_{\text{e}}^-}{\partial x}(t,1^-) = \frac{-L^- \hat{c}_{\text{e}}^-(t,1^-)}{P^*}, \tag{IV.9}$$

where $p_1(x)$ and p_{10} represent the observer gains as follows:

$$p_1(x) = -P_y(x,0), \tag{IV.10}$$

$$p_{10} = -\frac{\lambda}{2}. \tag{IV.11}$$

Observer gains are determined in Part 1 [9] such that $\hat{c}_e^-(t,0^-)$ converges to $c_e^-(t,0^-)$ as time approaches infinity.

Theorem 1. *Consider the normalized electrolyte lithium concentration PDEs in the negative electrode,* (IV.1)-(IV.3)*, and the designed observer* (IV.7)-(IV.11)*. For any initial condition under assumptions, if $\lambda \geq -\frac{1}{4}$ the designed observer* (IV.7)-(IV.9) *converges exponentially to the system* (IV.1)-(IV.3)*.*

C. Electrolyte observer for the positive electrode

The observer for the electrolyte lithium concentration in the positive electrode is designed as:

$$\frac{\partial \hat{c}_{\text{e}}^+}{\partial t}(t,x) = \frac{\partial^2 \hat{c}_{\text{e}}^+}{\partial x^2}(t,x) - \frac{L^+(1-t_c^0)}{D_{\text{e}}^{+,\text{eff}}F} I(t) + p_1(x)(c_{\text{e}}^+(t,0^+) - \hat{c}_{\text{e}}^+(t,0^+)), \tag{IV.12}$$

$$\frac{\partial \hat{c}_{\text{e}}^+}{\partial x}(t,0^+) = p_{10}(c_{\text{e}}^+(t,0^+) - \hat{c}_{\text{e}}^+(t,0^+)), \tag{IV.13}$$

$$\frac{\partial \hat{c}_{\text{e}}^+}{\partial x}(t,1^+) = \frac{L^+ \hat{c}_{\text{e}}^+(t,1^+)}{L^{\text{sep}} - P^*}, \tag{IV.14}$$

where $p_1(x)$ and p_{10} are the observer gains [9] chosen such that $\hat{c}_e^+(t,0^+)$ converges to $c_e^+(t,0^+)$ as time approaches infinity.

Theorem 2. *Consider the normalized electrolyte lithium concentration system in the positive electrode,* (IV.4)-(IV.6)*, and the corresponding state observer* (IV.12)-(IV.14)*. With the chosen gains for any initial condition under assumptions, if $\lambda \geq -\frac{1}{4}$, the designed observer* (IV.12)-(IV.14) *converges exponentially to the system* (IV.4)-(IV.6)*.*

Remark: The convergence proof and simulations of the electrolyte observer are included in Part 1 [9].

Authorized licensed use limited to: Texas Tech University. Downloaded on March 19,2025 at 15:03:30 UTC from IEEE Xplore. Restrictions apply.

V. Enhanced electrode lithium ion observer

A. Enhancing accuracy of estimated data for lithium concentration at the surface of the electrode particle $c_s^+(t, R_s^+)$

A.1 The enhanced voltage function

Based on the voltage equation in SPM (V.1), researchers utilized battery voltage as a measurement to determine the lithium concentration at the surface of the electrode particle $c_s^+(t, R_s^+)$ [19], [20]:

$$\begin{aligned} V(t) = &- \frac{RT}{\alpha_{a,c}F}\left[\sinh^{-1}\left(\frac{1}{2i_0^+(t)}\frac{I(t)}{a^+L^+}\right)\right. \\ &\left.+\sinh^{-1}\left(\frac{1}{2i_0^-(t)}\frac{I(t)}{a^-L^-}\right)\right] \\ &- \left(\frac{R_{\mathrm{f}}^+}{a^+L^+}+\frac{R_{\mathrm{f}}^-}{a^-L^-}\right)I(t) \\ &+ U^+\left(c_{\mathrm{ss}}^+(t)\right) - U^-\left(c_{\mathrm{ss}}^-(t)\right) \\ \triangleq &\, h_1\left(t, c_{\mathrm{ss}}^+(t), c_{\mathrm{ss}}^-(t), I(t)\right), \end{aligned} \tag{V.1}$$

where $c_{ss}^{\pm}(t) = c_s^{\pm}(t, R_s^{\pm})$. $\alpha_{a,c}$ and R represent the anodic/cathodic transfer coefficient and the universal gas constant, respectively. Additionally, $U^{\pm}(c_{ss}^{\pm}(t))$ and R_f denote the open-circuit potential and lumped resistance, respectively. In this model, voltage is a function of time, the lithium concentration at the particle's surface $c_{ss}^{\pm}(t)$, and the current $I(t)$. To simplify the voltage function (V.1), a relation between $c_{ss}^+(t)$ and $c_{ss}^-(t)$ is determined [20]:

$$\begin{aligned} c_{\mathrm{ss}}^-(t) = &\,\alpha\left(c_{\mathrm{ss}}^+(t) - \frac{8R_{\mathrm{s}}^+}{35}\bar{q}_{\mathrm{s}}^+(t) + \frac{R_{\mathrm{s}}^+}{35D_{\mathrm{s}}^+(t)}j^+(t)\right) + \beta \\ &+ \frac{8R_{\mathrm{s}}^-}{35}\bar{q}_{\mathrm{s}}^-(t) - \frac{R_{\mathrm{s}}^-}{35D_{\mathrm{s}}^-(t)}j^-(t). \end{aligned} \tag{V.2}$$

where $\alpha = -\frac{\varepsilon_s^+ L^+}{\varepsilon_s^- L^-}$ and $\beta = \frac{n_{\mathrm{Li,s}}}{\varepsilon_s^- L^-}$. $\varepsilon_s^{\pm}$ denotes the volume fraction in the solid phase, and $\bar{q}_s^{\pm}$ is derived from the polynomial solution profile, which can be found in [21]. From (V.2), a simplified form of the voltage function in (V.1) can be expressed as:

$$V(t) = h_2\left(t, c_{\mathrm{ss}}^+(t), I(t)\right). \tag{V.3}$$

In the enhanced model, SPMe [13], the voltage is defined as a function not only of the lithium concentration at the particle's surface but also of the electrolyte lithium concentration at the boundaries:

$$\begin{aligned} V(t) = &\left(U^+(\frac{c_{\mathrm{ss}}^+(t)}{c_{\mathrm{s}}^{+,\max}}) - U^-(\frac{c_{\mathrm{ss}}^-(t)}{c_{\mathrm{s}}^{-,\max}})\right) \\ &+ \left(\varphi_e^+(t,0^+) - \varphi_e^-(t,0^-)\right) \\ &+ \eta^+(t) + \eta_{\mathrm{shell}}^+(t) - \eta^-(t) - R_\Omega(t)I(t) \\ = &\, h\left(c_{\mathrm{ss}}^-(t), c_{\mathrm{ss}}^+(t), c_e^+(t,0^+), c_e^-(t,0^-), I(t)\right). \end{aligned} \tag{V.4}$$

Based on the voltage function derived in (V.3), a simplified expression for (V.4) can be written as:

$$V(t) = h\left(c_{\mathrm{ss}}^+(t), c_e^+(t,0^+), c_e^-(t,0^-), I(t)\right). \tag{V.5}$$

A.2 Inversion of voltage function

In this study, as detailed in Section IV, the electrolyte lithium-ion concentrations at the boundaries, $c_e^{\pm}(t, 0^{\pm})$, are derived from the measured electrolyte resistance using EIS. By employing these available parameters $c_e^{\pm}(t, 0^{\pm})$, including measured output voltage $V(t)$, a more precise estimation of the lithium concentration at the surface of the particle, $c_{ss}^+(t)$, can be achieved. As long as the function (V.5) is a one-to-one correspondence to $c_{ss}^+(t)$, uniformly in $I(t)$, one can invert it using the measured $V(t)$ and obtainable $c_e^{\pm}(t, 0^+)$, to derive the electrode concentration boundary condition in the positive electrode as follows:

$$c_{ss}^+(t) = h_0(V(t), c_e^+(t,0^+), c_e^-(t,0^-), I(t)). \tag{V.6}$$

B. Electrode lithium concentration observer

The electrode lithium concentration observer has been designed based on the following assumptions:

Assumption 2. *To obtain an output inversion function, the solid-phase concentration in the negative electrode was simplified by adopting a polynomial solution to represent the diffusion dynamics within the negative electrode [21].*

The lithium concentration in the positive and negative electrodes and the boundary are described as follows:

$$\frac{\partial c_s^{\pm}}{\partial t}(r,t) = \frac{1}{r^2}\frac{\partial}{\partial r}\left[D_s^{\pm}r^2\frac{\partial c_s^{\pm}}{\partial r}(r,t)\right], \tag{V.7}$$

$$\frac{\partial c_s^{\pm}}{\partial r}(0,t) = 0, \quad \frac{\partial c_s^{\pm}}{\partial r}(R_s^{\pm},t) = \pm\frac{1}{D_s^{\pm}Fa^{\pm}L^{\pm}}I(t). \tag{V.8}$$

The electrode observer for the lithium concentration in the positive electrode is designed as [13]:

$$\begin{aligned} \frac{\partial \hat{c}_s^+}{\partial t}(r,t) = &\, D_s^+\left[\frac{2}{r}\frac{\partial \hat{c}_s^+}{\partial r}(r,t) + \frac{\partial^2 \hat{c}_s^+}{\partial r^2}(r,t)\right] \\ &+ \bar{p}^+(r)\left[c_{\mathrm{ss}}^+(t) - \hat{c}_{\mathrm{ss}}^+(t)\right], \end{aligned} \tag{V.9}$$

$$\frac{\partial \hat{c}_s^+}{\partial r}(0,t) = 0, \tag{V.10}$$

$$\frac{\partial \hat{c}_s^+}{\partial r}\left(R_s^+,t\right) = \frac{I(t)}{D_s^+Fa^+L^+} + \bar{p}_0^+\left[c_{\mathrm{ss}}^+(t) - \hat{c}_{\mathrm{ss}}^+(t)\right]. \tag{V.11}$$

$$\bar{p}^+(r) = \frac{-\lambda D_s^+}{2R_s^+\bar{z}}\left[I_1(\bar{z}) - \frac{2\lambda}{\bar{z}}I_2(z)\right], \tag{V.12}$$

$$\bar{p}_0^+ = \frac{1}{2R_s^+}(3-\lambda), \quad \text{for } \lambda < \frac{1}{4}, \tag{V.13}$$

where $\bar{z} = \sqrt{\lambda\left(\frac{r^2}{(R_s^+)^2} - 1\right)}$ and $I_1(z)$ and $I_2(z)$ are the first and second-order modified Bessel functions of the first kind, respectively. The electrode observer for the lithium

Authorized licensed use limited to: Texas Tech University. Downloaded on March 19,2025 at 15:03:30 UTC from IEEE Xplore. Restrictions apply.

concentration in the negative electrode is designed as [13]:

$$\frac{\partial \hat{c}_s^-}{\partial t}(r,t) = D_s^- \left[\frac{2}{r}\frac{\partial \hat{c}_s^-}{\partial r}(r,t) + \frac{\partial^2 \hat{c}_s^-}{\partial r^2}(r,t)\right] + \bar{p}^-(r)\left[c_{\rm ss}^-(t) - \hat{c}_{\rm ss}^-(t)\right], \tag{V.14}$$

$$\frac{\partial \hat{c}_s^-}{\partial r}(0,t) = 0, \tag{V.15}$$

$$\frac{\partial \hat{c}_s^-}{\partial r}\left(R_s^-, t\right) = \frac{I(t)}{D_s^- F a^- L^-} + \bar{p}_0^-\left[c_{\rm ss}^-(t) - \hat{c}_{\rm ss}^-(t)\right]. \tag{V.16}$$

Observer gains for the negative electrode are designed as:

$$\bar{p}_0^- = -\frac{a^+ L^+ D_s^+}{a^- L^- D_s^-}\bar{p}_0^+, \tag{V.17}$$

$$\bar{p}^-(r) = -\frac{a^+ L^+}{\left(R_s^+\right)^2 \varepsilon_s^- L^-}\int_0^{R_s^+} r^2 \bar{p}^+(r) dr, \tag{V.18}$$

where $\varepsilon_s^- = 3/\left(a^- R_s^-\right)$.

Theorem 3. *For any initial value under Assumption 2, if* $\lambda < \frac{1}{4}$*, the proposed observer* (V.14)–(V.16) *converges to the corresponding system* (V.7)–(V.8)*.*

As this study primarily focuses on reverse sensitivity analysis, the simulation of the electrolyte observer is presented in Part 1 [9], and the simulation of the electrode observer will be addressed in a future journal version.

VI. Conclusion and Future Work

In this paper, a reverse sensitivity analysis is conducted on the lithium electrolyte concentration at the terminal boundaries of the negative and positive electrodes in lithium-ion batteries. This analysis is applied to three measurable parameters: electrolyte conductivity, electrolyte diffusion coefficient, and electrolyte resistance. An analytical derivation, a generic method, is employed for the sensitivity analysis approach. For the $LiFePO_4$ battery cell, electrolyte resistance is identified as the least sensitive parameter, while electrolyte conductivity emerges as the most sensitive. The findings can significantly benefit Part 1 of this study [9], by determining the most appropriate measurable parameter for obtaining the lithium electrolyte concentration at the boundaries when designing the electrolyte observer. Electrolyte resistance, being the least sensitive, is the most suitable choice for this purpose. Furthermore, this scheme can enhance the accuracy of electrode concentration estimation. Extending this method to various battery types and current profiles will be the focus of our future work. Additionally, incorporating the temperature effect into the analysis could also be considered for future enhancement. Experimental studies can also be performed to verify the proposed scheme.

References

[1] Vahid Safavi, Najmeh Bazmohammadi, Juan C Vasquez, and Josep M Guerrero. Battery state-of-health estimation: A step towards battery digital twins. *Electronics*, 13(3):587, 2024.

[2] Sadiqa Jafari and Yung Cheol Byun. Accurate remaining useful life estimation of lithium-ion batteries in electric vehicles based on a measurable feature-based approach with explainable ai. *The Journal of Supercomputing*, 80(4):4707–4732, 2024.

[3] Williams Agyei Appiah, Jonas Busk, Tejs Vegge, and Arghya Bhowmik. Sensitivity analysis methodology for battery degradation models. *Electrochimica Acta*, 439:141430, 2023.

[4] Joel C Forman, Scott J Moura, Jeffrey L Stein, and Hosam K Fathy. Genetic identification and fisher identifiability analysis of the doyle–fuller–newman model from experimental cycling of a lifepo4 cell. *Journal of Power Sources*, 210:263–275, 2012.

[5] Vishvak Kannan, Adrian Fisher, and Erik Birgersson. Monte carlo assisted sensitivity analysis of a li-ion battery with a phase change material. *Journal of Energy Storage*, 35:102269, 2021.

[6] Qingzhi Lai, Sidharth Jangra, Hyoung Jun Ahn, Geumbee Kim, Won Tae Joe, and Xinfan Lin. Analytical derivation and analysis of parameter sensitivity for battery electrochemical dynamics. *Journal of Power Sources*, 472:228338, 2020.

[7] Sara Sepasiahooyi and Shu-Xia Tang. Sensitivity analysis of lithium-ion battery soh indicators: An analytical study. In *2024 American Control Conference (ACC)*, pages 1971–1976. IEEE, 2024.

[8] Jiahuan Tong, Shengli Wu, Nicolas Von Solms, Xiaodong Liang, Feng Huo, Qing Zhou, Hongyan He, and Suojiang Zhang. The effect of concentration of lithium salt on the structural and transport properties of ionic liquid-based electrolytes. *Frontiers in chemistry*, 7:945, 2020.

[9] Sara Sepasiahooyi and Shu-Xia Tang. Enhanced battery state estimation: Part 1 -electrolyte lithium-ion concentration observer. In *Conference on Decision and Control*. IEEE, 2024.

[10] Weihan Li, Decheng Cao, Dominik Jöst, Florian Ringbeck, Matthias Kuipers, Fabian Frie, and Dirk Uwe Sauer. Parameter sensitivity analysis of electrochemical model-based battery management systems for lithium-ion batteries. *Applied Energy*, 269:115104, 2020.

[11] Johannes Landesfeind and Hubert A Gasteiger. Temperature and concentration dependence of the ionic transport properties of lithium-ion battery electrolytes. *Journal of The Electrochemical Society*, 166(14):A3079–A3097, 2019.

[12] Madeleine Ecker, Thi Kim Dung Tran, Philipp Dechent, Stefan Käbitz, Alexander Warnecke, and Dirk Uwe Sauer. Parameterization of a physico-chemical model of a lithium-ion battery: I. determination of parameters. *Journal of The Electrochemical Society*, 162(9):A1836, 2015.

[13] Scott J Moura, Federico Bribiesca Argomedo, Reinhardt Klein, Anahita Mirtabatabaei, and Miroslav Krstic. Battery state estimation for a single particle model with electrolyte dynamics. *IEEE Transactions on Control Systems Technology*, 25(2):453–468, 2016.

[14] Clément Edouard, Martin Petit, C Forgez, Julien Bernard, and Renaud Revel. Parameter sensitivity analysis of a simplified electrochemical and thermal model for li-ion batteries aging. *Journal of Power Sources*, 325:482–494, 2016.

[15] Weida Toh Zuchang Gao Junbo Jia Joel Chiew, Cheng Chin and Caizhi Zhang. A pseudo three-dimensional electrochemical-thermal model of a cylindrical LiFePO4/graphite battery. *Applied Thermal Engineering*, 147:450–463, 2019.

[16] Wenxiu Wang, Daniel Juarez-Robles, and Partha P Mukherjee. Electroanalytical quantification of electrolyte transport resistance in porous electrodes. *Journal of The Electrochemical Society*, 167(8):080510, 2020.

[17] Alexandros Ch Lazanas and Mamas I Prodromidis. Electrochemical impedance spectroscopy a tutorial. *ACS Measurement Science Au*, 2023.

[18] Kaixin Cui, Shu-Xia Tang, Yuan Huang, Hao Yu, and Dawei Shi. Event-triggered active disturbance rejection control for a class of networked systems with unmatched uncertainties: Theoretic and experimental results. *Control Engineering Practice*, 115:104907, 2021.

[19] Scott J Moura, Nalin A Chaturvedi, and Miroslav Krstić. Adaptive partial differential equation observer for battery state-of-charge/state-of-health estimation via an electrochemical model. *Journal of Dynamic Systems, Measurement, and Control*, 136(1):011–015, 2014.

[20] Shu-Xia Tang, Leobardo Camacho-Solorio, Yebin Wang, and Miroslav Krstic. State-of-charge estimation from a thermal–electrochemical model of lithium-ion batteries. *Automatica*, 83:206–219, 2017.

[21] Venkat R Subramanian, Vinten D Diwakar, and Deepak Tapriyal. Efficient macro-micro scale coupled modeling of batteries. *Journal of The Electrochemical Society*, 152(10):A2002, 2005.

Authorized licensed use limited to: Texas Tech University. Downloaded on March 19,2025 at 15:03:30 UTC from IEEE Xplore. Restrictions apply.